Journal of Non-Crystalline Solids 371–372 (2013) 14–21

Contents lists available at SciVerse ScienceDirect

Journal of Non-Crystalline Solids

journal homepage: www.elsevier.com/ locate/ jnoncrysol

Optical absorption and structural studies of bismuth borate glasses containing Er^{3+} ions

M. Farouk [a,c,*], A. Samir [b], F. Metawe [b], M. Elokr [a]

[a] Physics Department, Faculty of Science, Al Azhar University, Nasr City, Cairo 11884, Egypt
[b] Engineering, Mathematics, and Physics Department, Faculty of Engineering, Benha University, Egypt
[c] Department of Physics, Faculty of Science, Jazan University, Saudi Arabia

ARTICLE INFO

Article history:
Received 6 February 2013
Received in revised form 27 March 2013
Available online 7 May 2013

Keywords:
Bismuthate glasses;
Optical absorption;
DSC;
IR spectroscopy

ABSTRACT

Glasses with composition xBi_2O_3–$24Na_2O$–$(75 - x)B_2O_3$–$1Er_2O_3$ (where x = 0, 5, 10, 15, 25, 33, 40 mol%), were prepared by the melt quenching technique. The effect of Bi_2O_3 content on thermal stability, optical properties and structures of these glasses is systematically investigated by X-ray diffraction, infrared spectroscopy and DTA techniques. The variations in the optical band gap energies, with Bi_2O_3 content have been discussed in terms of changes in the glass structure. Urbach energy increases with increasing Bi_2O_3 content in the present glass system. It is found that the density, molar volume and optical basicity increase with increasing Bi_2O_3. The glass transition temperature (T_g) of the samples was found to decrease with the Bi_2O_3 content. IR measurements revealed an existence of trigonal BO_3 pyramid, tetrahedron BO_4, pyramidal BiO_3 and octahedron BiO_6 structural units in the network of the investigated glass. Furthermore, a decrease in BO_4 and an increase in BO_3 take place against the increase of x which means that, Bi_2O_3 plays the role of network modifier in the structural network.

1. Introduction

Recently, glasses formed with heavy metal ions have received significant attention because of their interesting optical applications. These glasses are better competitors for optical transmission studies due to their long infrared (IR) cut-off [1,2]. On the other hand, the heavy metal oxide glasses such as; the bismuthate glasses have attracted an important interest for optoelectronic and photonic applications because of their important properties such as higher refractive indices (>2.0), the optical nonlinearities and transmission at longer wavelengths in the infrared region. Due to these properties, the use of the mentioned glasses provides the possibility of developing more efficient lasers and fiber optic amplifiers [3–5]. In terms of the crystalline configuration, Bi_2O_3 is an oxide having a high valence cation of low field strength and high polarizability. So, its glassy phase cannot conventionally be compared with pure B_2O_3 glass. Bi_2O_3 like ZnO can occupy both network-forming and network modifying positions in the borate network glasses and, as a result, the physical properties of such glasses exhibit discontinuous changes, when the structural role of the cation changes [6]. Bismuth oxide cannot be considered as network former due to small field strength of Bi^{3+} ion. However, in the presence of conventional glass formers such as B_2O_3 glass formation is possible. Bismuth form Bi_2O_3 generally tends to occupy octahedral positions in the glass structure. The additional oxygen required for octahedral coordination of Bi is provided by the oxygen atoms in the host matrix through non-bonding coordination, because Bi_2O_3 by itself can only give rise to $[BiO_{3/2}]^0$ units [7]. Glasses based on heavy metal oxide such as Bi_2O_3 have wide applications in the field of glass ceramics, layers for optical and electronic devices, thermal and mechanical sensors, reflecting windows, etc. [8]. Boric oxide, B_2O_3, acts as one of the most important glass formers and flux materials.

Melts with compositions rich in B_2O_3 exhibit rather high viscosity and tend to the formation of glasses. In crystalline form, on the other hand, borates with various compositions are of exceptional importance due to their interesting linear and nonlinear optical properties.

The boron atom usually coordinates with either three or four oxygen atoms forming $[BO_3]^{3-}$ or $[BO_4]^{5-}$ structural units. Furthermore, these two fundamental units can be arbitrarily combined to form different B_xO_y structural groups. Among these borates, especially the monoclinic bismuth borate BiB_3O_6 shows up remarkably large linear and nonlinear optical coefficients [8–10]. The structure of borate glasses is particularly interesting because of the so-called boron anomaly and variety of skeleton modification and owing to influence of non-bridging oxygen or M – O bonds on the optical properties of the glasses [11].

Rare earth ions containing special 4f electrons that are capable of excitation can greatly improve the nonlinear optical properties of glasses; consequently, the use of these ions can contribute to the development of the applications of optical materials. Glasses doped with Nd^{3+}, Er^{3+}, Sm^{3+}, and La^{3+} have also been reported and are regarded as excellent laser materials. Although these glasses are considered to be promising materials for use in all-optical devices, it is required for them to possess high thermal stability, excellent surface polishing properties, high refractive index, etc. [2,12–14]. It is therefore important to carefully prepare and measure the density, glass transition temperature (T_g) values and

* Corresponding author at: Physics Department, Faculty of Science, Al Azhar University, Nasr City, Cairo 11884, Egypt. Tel.: +20 966558639371; fax: +20 2 22 629356.
E-mail address: mf_egypt22375@yahoo.com (M. Farouk).

0022-3093/$ – see front matter © 2013 Elsevier B.V. All rights reserved.
http://dx.doi.org/10.1016/j.jnoncrysol.2013.04.001

calculate N_4 (BO_4 / (BO_3 + BO_4)) from IR spectra in these technologically important materials. Borate glasses unlike silicates show two coordination numbers of 3 and 4 with oxygen and it is known that, N_4 is the single most important parameter that is required for the accurate modeling of glass structure.

2. Experimental setup

2.1. Glass preparation

Glass system of composition xBi_2O_3–$24Na_2O$–$(75 - x)B_2O_3$–$1Er_2O_3$ (where x = 0, 5, 10, 15, 25, 33, 40 mol%). Samples have been prepared using reagent grade materials. The starting materials used were: Bi_2O_3, Na_2CO_3, and H_3BO_3 all with 99.9% purity and Er_2O_3 with 99.99% purity. Glass samples were prepared by conventional melt-quenching technique. Each composition was taken in an open porcelain crucible and melted in an electric furnace at the temperature range 850–1100 °C for 1–2 h depending on glass composition. The crucible was shaken frequently for the homogeneous mixing of all the constituents. Finally the molten liquid was poured and pressed between two preheated brass plates. The bismuth free sample is pink and the samples containing bismuth have yellow color which becomes deep in color with increasing bismuth content.

2.2. Glass characterization

X-ray diffraction patterns were recorded to check the non-crystallinity of the prepared glass samples using advance XRD diffractometer Bruker AXS D8. The patterns revealed a broad hump that characterizes the amorphous materials, and did not reveal any sharp peaks indicating the non-crystalline nature of the prepared glasses as shown in Fig. 1. The optical absorption spectra of the glass samples were recorded at room temperature using a JENWAY6405UV/Vis Spectrophotometer in the wavelength range 190–1100 nm. The density was measured at room temperature using the Archimedes method with carbon tetrachloride as the immersion liquid. The density is calculated according to the formula:

$$\rho = [w_a/(w_a - w_b)]x\,\rho_o \quad (1)$$

where w_a is the weight of the glass sample measured in air, w_b is the weight when the glass is immersed in liquid and ρ_o is the density of carbon tetrachloride. The molar volume (V_M) was calculated using the relation $V_M = M_w/\rho$, where M_w is the total molecular weight of the multicomponent sample. The glass transition temperature T_g of the samples was determined by differential-scanning calorimeter (DSC) [a SETARAM Labsys TM TG-DSC16 thermal analyzer], at a heating rate of 10 °C/min. The glass transition temperature (T_g) values are evaluated from the slopes of DSC curves. The IR absorption spectra of the glasses were recorded, at room temperature in the wave number range of 400–2000 cm^{-1} by a Bruker, single beam spectrometer with a resolution of 2 cm^{-1}, using the KBr disk technique. The infrared spectra were corrected for the dark current noises, and normalized to eliminate the concentration effect of the powder sample in the KBr disk. The obtained spectra were deconvoluted to enable shedding further light on the structural changes of BO_3 triangles and BO_4 tetrahedra, as they are the basic units in these glasses.

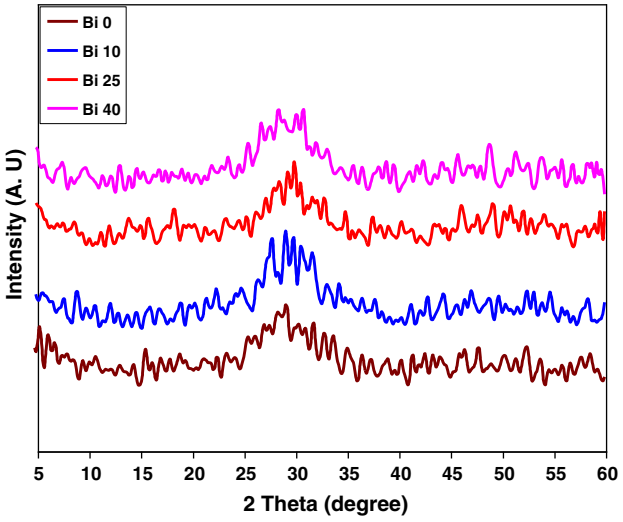

Fig. 1. X-ray pattern for glass samples.

3. Results and discussion

3.1. Optical absorption studies

The optical absorption spectra of Er^{3+} doped sodium bismuth borate glasses in the UV-visible (190–1100 nm) region are shown in Fig. 2. An absorption edge is clearly observed in the UV region. It exhibits blue shift by increasing Bi_2O_3 concentration. The spectra consist of a set of absorption bands which is a characteristic of Er^{+3}. Such bands arise from the intra-configurational (f–f) transition from the ground state of Er^{3+} ions to various excited states. The detected peaks exhibit no shift. This is expected since in the rare earth elements L–S coupling is dominant and shields the inner electrons i.e. we are dealing with almost free ions. In this respect the 4f electrons are shielded by the outer 5s and 5p bonding electrons, which leads to sharp absorption and emission bands [15,16].

The analysis of the optical absorption spectra of Fig. 2, reveals that, all samples follow common pattern, where an absorption edge is observed, the position of which depends on composition. The optical absorption edge extended over wide wavelength range i.e. no sharp edge (Urbach edge), which indicates the amorphous nature of the prepared samples. This is inconsistent with the data obtained from XRD. Generally, it is accepted that the absorption edge depends on the oxygen bond strength in the glass forming network. The obtained data indicate a change in oxygen bond strength in the glass network, such change affects the absorption characteristics of the investigated samples. The absorption coefficient was calculated from the formula [17]:

$$\alpha = \left(\frac{1}{d}\right)\ln\left(\frac{I_0}{I}\right) = 2.303\frac{A}{d} \quad (2)$$

where I_o and I are the intensities of the incident and transmitted beams, respectively and d corresponds to thickness of each sample. The factor $\ln(I_0/I)$ is the absorbance.

The higher energy parts of the spectra particularly those associated with the integrand electronic transition will provide further information about the electronic states. In this respect, the electrons are excited from a filled band to an empty one by photon absorption and as a consequence a marked increase in the absorption coefficient $\alpha(\omega)$ will result. The onset of this rapid change in $\alpha(\omega)$ is called fundamental absorption edge and the corresponding energy is defined as the energy gap. The relation between $\alpha(\omega)$ and the photon energy of the incident radiation, ω was interpreted by Davis and Mott [17] and can be written in general form as:

$$\alpha(\omega) = \left[B\left(h\omega - E_g\right)^n\right]/h\omega \quad (3)$$

where B is constant called band tailing parameter, E_g is the energy of the optical band gap, n depends on the type of transition (direct or indirect) taking the values n = 2, 3, 1/2, and 1/3 which correspond to indirect allowed, indirect forbidden, direct allowed, and direct forbidden transitions respectively, n depends also on the nature of the material (crystal

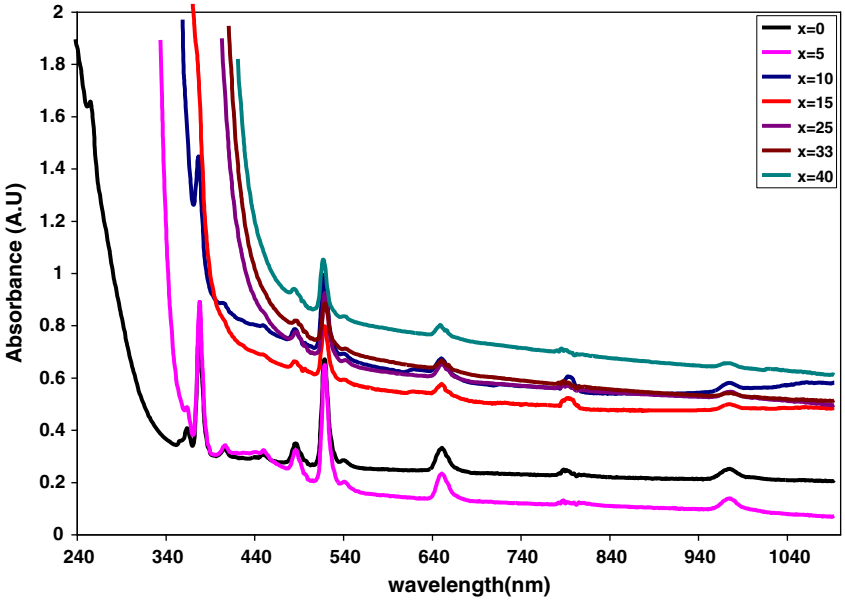

Fig. 2. Absorbance versus wavelength of glass system as a function of the Bi_2O_3 content.

or amorphous). For amorphous materials, indirect transitions are valid according to Tauc relation, i.e. the power part n = 2. By plotting $(\alpha\,\omega)^{1/2}$ as a function of photon energy ω, the optical energy band gap (E_g) can be determined by extrapolating the linear region of the curve to the (ω) axis where $(\alpha\,\omega)^{1/2} = 0$ as shown in Fig. 3, and their values are in Table 1.

The relation between α(ω) and Urbach energy (ΔE) is given by the well known Urbach relation[18]:

$$\alpha(\omega) = \alpha_o \exp[h\omega/\Delta E] \quad (4)$$

where α_0 is constant and ΔE is usually interpreted as the width of the tail of the localized states in the band gap and hυ is the incident photon energy. The natural logarithm of absorption coefficients, lnα, is plotted against photon energy, ω, which is shown in Fig. 4, as an example. The values of Urbach energy (ΔE) were calculated by determining the slopes of the linear portion of the curves and taking their reciprocals. The values of ΔE are listed in Table 1. It is found that, Urbach energy ΔE increases with increasing Bi_2O_3 content in glass samples. This may indicate that the addition of Bi increases the disorder of glass systems.

A plot of Eg and ΔE against Bi_2O_3 content shows that E_g decreases linearly and ΔE increases linearly with increasing Bi_2O_3 content, as shown in Fig. 5. The decreasing values of E_g by increasing the Bi_2O_3 content can be understood in terms of the structural changes that are taking place. In literature, boron and bismuth are known to have more than one stable configuration, i.e., boron triangles and tetraborate for boron and bismuth pyramidal and octahedral units for bismuth. Therefore, as discussed previously, increasing the Bi_2O_3 content increases the bond length of the BO_3 structural units, which in turn is in direct proportionality to the molar volume, and also creates more NBO. These factors, besides the weaker bond strength of Bi – O (80.3 kcal/mol) compared

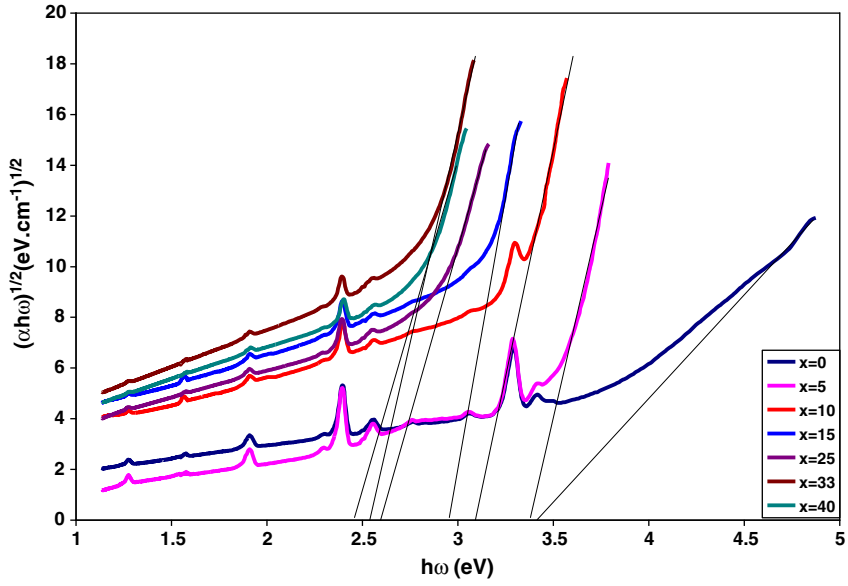

Fig. 3. $(\alpha\,\omega)^{1/2}$ as a function of ω for the present glass system.

Table 1
Various physical properties of the prepared samples.

Physical parameters	Bi_2O_3 (x mol%)						
	x = 0	x = 5	x = 10	x = 15	x = 25	x = 33	x = 40
Density (g/cm^3)	2.35	2.93	3.51	4.05	4.74	5.32	5.74
Molar volume (cm^3/mol)	30.10	30.90	31.47	32.17	35.79	37.85	39.92
Oxygen packing density (g-atom/l)	93.00	90.53	88.96	87.20	78.21	73.95	70.12
Ion concentration ($N \times 10^{22}$ (ions/cm^3))	1.99	1.94	1.91	1.87	1.68	1.59	1.50
Average site separation $\times 10^{-8}$ (cm)	1.48	1.49	1.50	1.51	1.57	1.60	1.63
Field strength $\times 10^{16}$ (cm^{-2})	1.36	1.33	1.32	1.30	1.21	1.16	1.12
Electronegativity (χ_{2av})	2.6094	2.6090	2.6086	2.6082	2.6074	2.6068	2.6062
Electronic polarizability (α_o^{2-})	1.5559	1.5562	1.5565	1.5567	1.5573	1.5577	1.5581
Optical basicity (Λ)	0.5955	0.5557	0.5559	0.5560	0.5564	0.5567	0.5570
glass transition temperature (T_g)	460	443	440	408	391	416	405
Optical band gap (E_g) (eV)	3.45	3.4	3.1	2.95	2.6	2.55	2.45
Urbach energy (ΔE) (eV)	0.13	0.14	0.18	0.21	0.22	0.24	0.26

to the bond strength of B–O (192.7 kcal/mol), are responsible for the decrease of E_g values [19,20].

3.2. Density, molar volume, oxygen packing density and glass transition temperature

The values of the measured density (ρ) and the calculated molar volume (V_M) are listed in Table 1. Fig. 6, shows the variation of density and molar volume with bismuth oxide (Bi_2O_3) content. The obtained results reveal that, the density increases linearly from 2.35 to 5.74 g/cm^3, and the molar volume increases linearly from 30.01 to 39.92 cm^3/mol as the Bi_2O_3 content increases at the expense of the B_2O_3 content, the density values of the studied glasses are higher than the density value for pure B_2O_3 (1838 kg/m^3), which agrees with the data reported elsewhere [21]. The increase in the density by increasing the modifier is most likely related to the replacement of B_2O_3 (atomic mass 69.62) by Bi_2O_3 (atomic mass 465.95). In short, the increase in density of the glasses accompanying the addition of Bi_2O_3 is probably attributable to a change in cross-link density and coordination numbers of Bi^{3+} ions. The density is a powerful tool, capable of studying the changes in the structure of glasses. It depends on compactness, geometrical configurations, co-ordination numbers, cross-link densities, and dimensions of interstitial spaces of the glass. Thus, replacement of light elements by heavy ones in the glass leads to a linear variation. Therefore, the density of glass samples increases linearly, that has a linear dependence on the compositions [21].

In general, it is expected that the density and the molar volume should show opposite behavior to each other, but in the present glasses the behavior is different. However, this anomalous behavior was reported earlier for many glass systems [21–23]. Such behavior allows us to conclude that the addition of Bi_2O_3 leads to the formation of non-bridging oxygen (NBOs) and expands (opens up) the structure of the loose network of the base glass sample $24Na_2O–75B_2O_3–1Er_2O_3$ (mol%). The larger values of the radii and bond length of Bi_2O_3, compared to those of B_2O_3, resulted in a formation of excess free volume, which increases the overall molar volume of these glasses. This trend supports the so-called open structure concept [21].

Oxygen packing density (OPD) which is a measure of the tightness of packing of the oxide network can be calculated using molecular weight (M_w), and density (ρ) through the following relation [7]:

$$O = \left[\frac{\rho}{M_W}\right] \times n \tag{5}$$

where n is the number of oxygen atoms per formula unit. Table 1, and Fig. 7, show the dependence of OPD on Bi_2O_3 content. It can be seen in Fig. 7, that OPD decreases as the concentration of Bi_2O_3 content increases. This indicates that the structure becomes loosely packed and the degree of disorder increases as Bi_2O_3 content increased. A looser macromolecular structure requires smaller internal energy for the chain mobility which is needed for the glass transition. Thus, the addition of Bi_2O_3 indicates the formation of a more open macromolecular chain in the present glass system leading to a decrease in T_g [7,23].

The Er-ion concentration (N) is of great interest since it affects different properties of the host material. The number of ions per cubic centimeter was calculated according to the formula [24,25]

$$N\left(\text{ion/cm}^3\right) = \frac{x\rho N_A}{M_W} \tag{6}$$

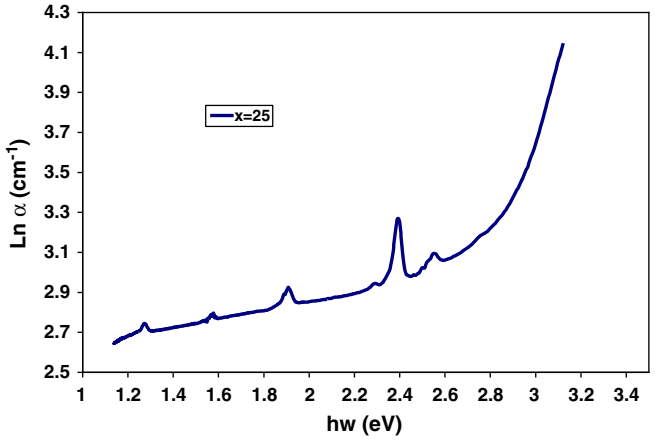

Fig. 4. Urbach plot of x = 25 mol% as an example.

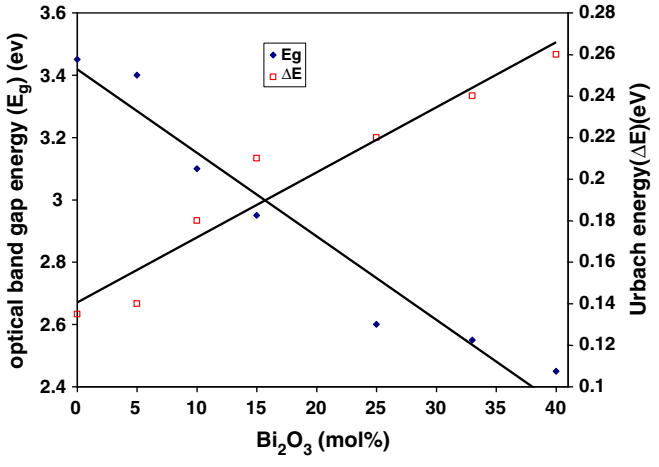

Fig. 5. The variation of Optical band gap (E_g) and Urbach energy (ΔE) with Bi_2O_3 content.

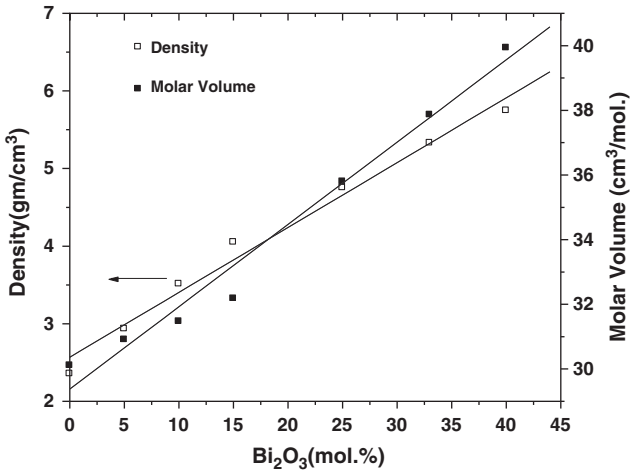

Fig. 6. Variation of the density and the molar volume of glasses as a function of the Bi_2O_3 content.

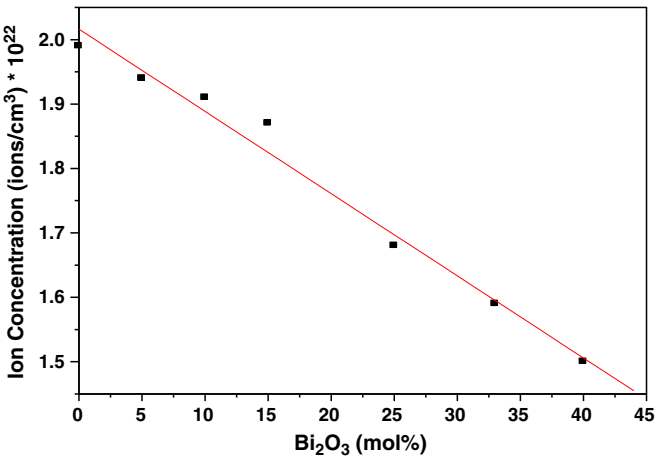

Fig. 8. Composition dependence of rare earth ion concentration (N) on Bi_2O_3 content.

where N_A is Avogadro's number, and x is the mol fraction of rare earth oxide. The calculated values are listed in Table 1, and shown in Fig. 8. The data reveal that Er-ion concentration decreases as Bi_2O_3 increased, this is most likely due to the change in density.

The field strength, F, of Er^{3+} ion is calculated by: $F = Z / r_p^2$ where Z is the valence of Er ion and r_p is its average site separation and is given by $r_p(A^0) = 1/2[\pi / 6\ N]^{1/3}$ as described in [25]. The calculated values are given in Table 1, and are shown in Fig. 9. In general, the average ion separation and the field strength should show opposite trend which is clearly observed in the present work. The value of average rare earth ion separation (r_p) increases with increasing Bi_2O_3 content. This can be attributed to the open structure caused by Bi_2O_3 addition, and the value of the field strength (F) decreases with increasing Bi_2O_3 content i.e. the results follow the normal behavior, where average RE–O distance increases producing a weaker field around the Er^{3+} ions.

DSC is used to characterize the glasses and to determine glass transition temperature (T_g), which is useful in suggesting structural changes that take place by the compositional changes. This is because T_g is very sensitive to any change of the coordination number of the network-forming atoms and also to the formation of non-bridging oxygens. Glass transition temperature (T_g) can also be considered as an index of glass structure in a certain extent. Fig. 10, shows the DSC curve of x = 15 mol%. In the glass system all the samples exhibited an endothermic peak due to the glass transition temperature and the observed T_g lies in Table 1. As shown (inset in Fig. 10), it is observed that, the glass transition temperature varies non-linearly with Bi_2O_3 content. There is a decreasing trend in T_g with the increasing content of Bi_2O_3 up to 25 mol%, and for further increase a decreasing trend could be visualized. It has been reported that, the T_g is strictly related to the density of cross-linking, the tightness of the network formers and the coordination number of the network-forming atoms. Therefore, it is suggested that, the decrease in T_g up to 25 mol% of Bi_2O_3 content is due to the increase in the number of Bi–O linkages, which are weaker than B–O linkages leading to the decrease in the density of cross-linking of the bismuthate glass network. Thus, Bi–O–Bi cross-linkages that were broken to form non-bridging oxygen in the glasses result in the decrease of T_g. But beyond 25 mol%, the increasing trend in the T_g may be due to small decrease in the number of non-bridging oxygen ions and is also associated with the formation of BO_4 tetrahedra. Therefore, the non-linear variation of T_g with Bi_2O_3 content is due to the creation and variation in $N_4(BO_4 / (BO_3 + BO_4))$ units, and to some extent bridging and non-bridging oxygen ions (as seen in IR spectra) [19,26,28,23].

3.3. Electronic polarizability (α_0^{2-}) and optical basicity (Λ)

The optical basicity and the average electronic polarizability of ions have been successfully used to relate the physical properties of a glass

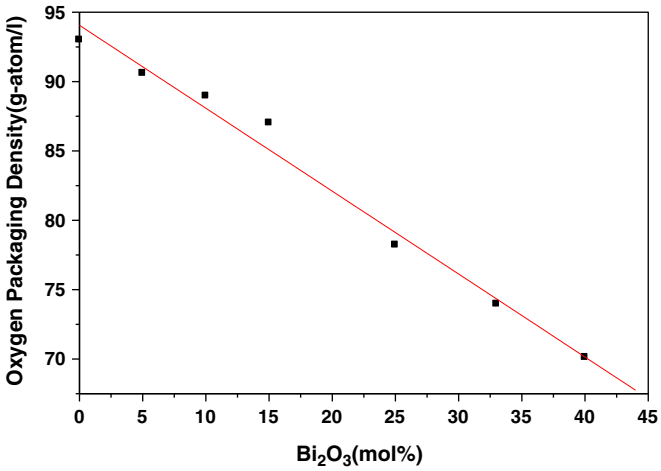

Fig. 7. Dependence of oxygen packing density (OPD) on Bi_2O_3 content.

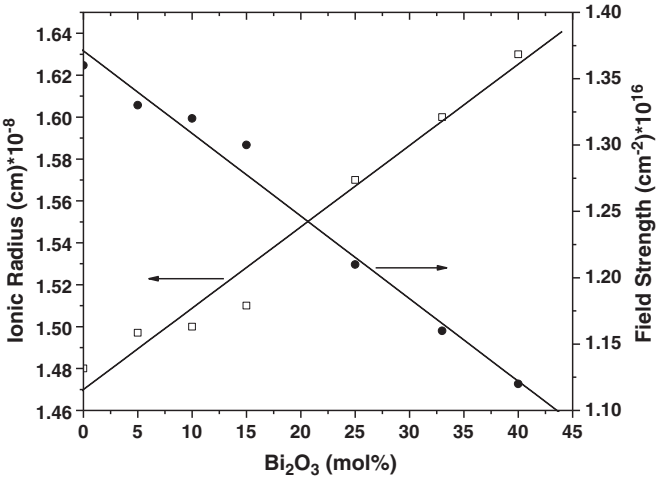

Fig. 9. Dependence of ionic radius (r_p) and the field strength (F) on Bi_2O_3 content.

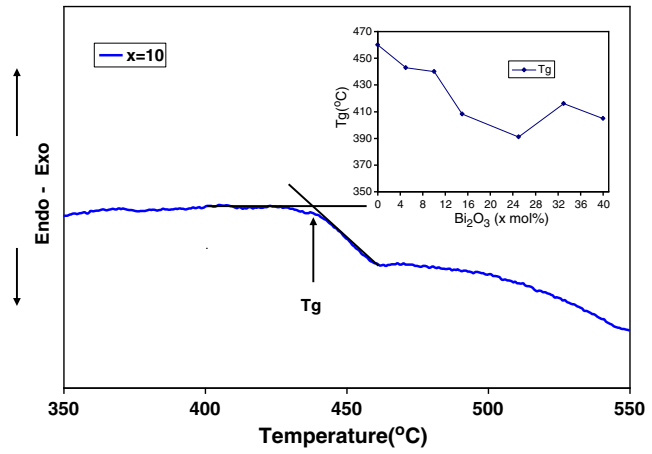

Fig. 10. DSC curve of x = 10 mol% as an example and inset representing glass transition temperature with Bi_2O_3 mol%.

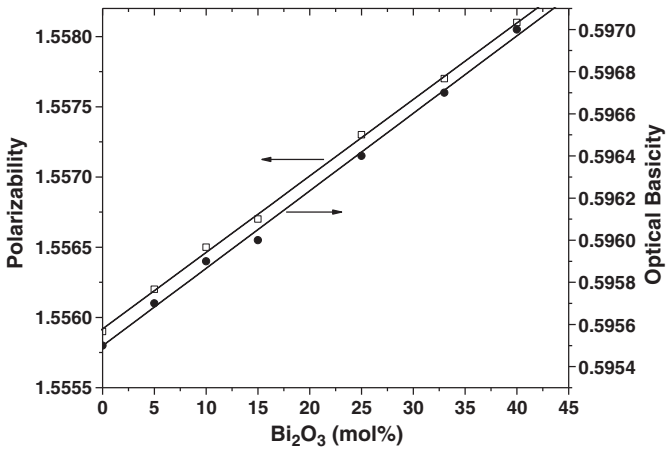

Fig. 11. Composition dependence of polarizability and the optical basicity.

with its structure [22]. The average electronic polarizability of ions is considered to be one of the most important properties of materials, which is closely related to their applicability in the field of optics and electronics [29]. The optical basicity proposed by Duffy and Ingram [30,31], was used as a measure of acid–base properties of the oxide glasses and is expressed in terms of the electron density carried by oxygen. The optical basicity of an oxide glass can be conventionally measured in terms of the ability of glass to donate negative charge to the probe ion [32,33]. In the present work, the empirical relations are derived for the average electronic polarizability (α_0^{2-}) and optical basicity (Λ) from Duffy [30,34,35], for the four-oxide glasses Na_2O, B_2O_3, Bi_2O_3, and Er_2O_3. The calculated values of the optical basicity, Λ, as well as the electronic polarizability, α_0^{2-}, are listed in Table 1, and depicted in Fig. 11. Both electronic polarizability and optical basicity are increased linearly by increasing Bi_2O_3 content. This is mainly due to the fact that Bi_2O_3 has a higher polarizability and higher optical basicity (due to its larger ionic radii) than Na_2O, Er_2O_3 and B_2O_3. The basicity increases with the increase in polarizability. It is well known in the literature that Bi^{3+} ions are highly polarizable. Therefore, the increase in Bi_2O_3 content causes an increase in optical basicity in these glasses. The change of optical basicity is very small by increasing Bi_2O_3 content from x = 0 to 40 mol%. This can be accounted by considering the values of the electronegativity of B (2.04) and Bi (2.02), which give almost equal values of the oxide basicity.

3.4. Infrared spectral studies

Infrared spectroscopy is usually used to obtain the essential information concerning the arrangement of the structural units of the studied glasses. It is assumed that the vibrations of structural units of the glass network are independent of the vibration of the other neighboring units [14]. The infrared absorption spectra for the glass samples are shown in Fig. 12.

The vibrational modes of the borate network are seen to be mainly active in the three infrared spectral regions, which are similar to those reported by several workers [36,37]. The first group of bands, which occurs at 1200–1600 cm^{-1}, is due to the asymmetric stretching vibration of the B – O band of trigonal BO_3 units. The second group lies between 800 and 1200 cm^{-1} and is due to the B – O bond stretching of the tetrahedral BO_4 units. The third group is usually observed around 700 cm^{-1} and is due to the bending of B – O – B in [BO_3] trigonal [33]. The glasses containing Bi_2O_3 have four fundamental vibrations in the IR spectral regions at ~830, ~620, ~450, and ~350 cm^{-1} [37]. Three broad bands are observed around 700, 900 and 1300 cm^{-1} for all investigated samples. By addition of Bi_2O_3 a fourth band starts to appear around 520 cm^{-1} and is clearly observed in samples (x = 15, 25, 33, 40 mol%) and its intensity increases as shown in Fig. 12. The spectra show little variation in the center of the band around 700 cm^{-1}, while, the center of the bands around 900 and 1300 cm^{-1} is shifted to lower wave number i.e. exhibits red shift and their width become wider as the Bi_2O_3 content increased. The obtained broad bands may confirm the amorphous nature of the studied samples and are in agreement with X-ray measurements [38–40]. The observed band around 700 cm^{-1} is attributed to the bending vibration of B – O – B linkages of BO_3 units [7,12,41,42]. This band shows a tendency to shift towards higher wave number (blue shift). This means that the bond strength is increased and bond length is decreased. In this respect the compactness of the structure units should be increased. This factor with the difference in atomic weights of Bi and B is responsible for the increased density by increasing the Bi_2O_3 content. Such effects cause change in free volume. This confirms the explanation given for the density and molar volume behavior. The strongest absorption bands of the borate glass located in the range of 1260 to 1540 cm^{-1} are usually attributed to B – O symmetric stretching of [BO_3] group. The absorption bands that lie in the range from 900 to 1120 cm^{-1} are assigned to B – O stretching of [BO_4] units and overlapping with vibrations of NBOs in BO_4 units [43]. The infrared spectra showed that the addition of Bi_2O_3 that causes a broad absorption band arises in the region from 850 to 1100 cm^{-1}. Bands in this region are not observed in the infrared spectra of pure B_2O_3 glass. It was reported that glasses containing sufficiently high concentrations of Bi_2O_3 have an absorption bands in the range of 750

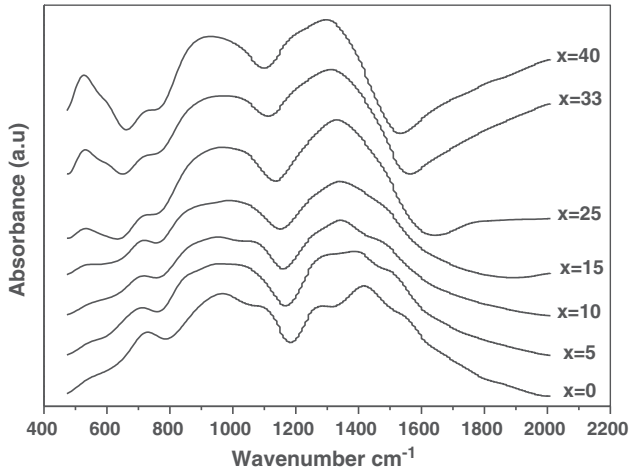

Fig. 12. The IR spectra of the prepared samples.

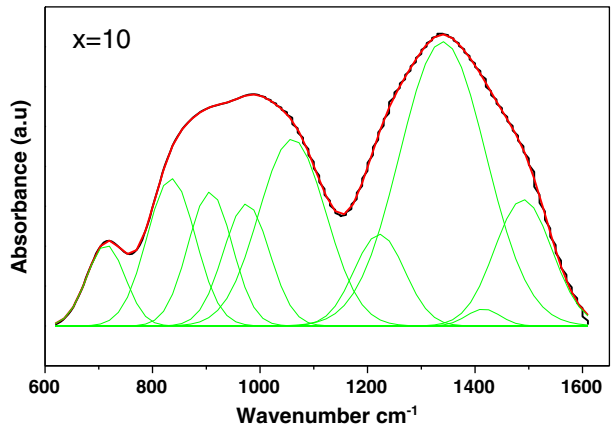

Fig. 13. The deconvoluted IR spectrum for x = 15 as an example.

to 900 cm^{-1}, which are attributed to stretching vibrations of Bi – O in BiO_3 units. The most important condition for the existence of $[BiO_3]$ polyhedra is the presence of a band around 830 cm^{-1} in the infrared spectra.

The absence of this band in the infrared spectra proves that only $[BiO_6]$ octahedral is the main structural unit [12]. In the studied glasses, the IR features located below 600 cm^{-1} are attributed to Bi – O vibrations in $[BiO_6]$ so the band observed at 520 cm^{-1} is attributed to the õvibration of $[BiO_6]$ [12]. The intensity of this band increases with increasing Bi_2O_3 content. To get precise information about the structural groups in glass, the spectra have been deconvoluted, this was made by using the Spectra Manager program assuming Gaussian type function that allows better identification of the absorption bands that appear in these spectra in order to perform their assignment [14]. Fig. 13, illustrated the results of the deconvolution for x = 10 mol%.

The obtained broad bands are a result of the overlapping of some individual bands. Each individual band has its characteristic parameters such as its center, which is related to some type of vibrations of a specific structural group, and its relative area, which is proportional to the concentration of this structural group [21]. These characteristic parameters can be used to calculate the fraction N_4 of BO_4 units in the borate matrix for each composition. N_4 can be defined as the ratio of the concentration of BO_4 units to the concentration of $(BO_3 + BO_4)$ units [44,14]. From Fig. 14, it is clear that, N_4 decreases in the first five samples .i.e. the BO_4 decreases and BO_3 increases, this means that Bi_2O_3 enters the network as a glass modifier. But in the samples (x = 33, 40 mol%) BO_4 increases and BO_3 decreases this means that Bi_2O_3 enters the network as a glass former. Therefore, it can be accepted that the content of $[BO_4]$ is relatively higher in sample (x = 33, 40 mol%). It is observed that, there are no obtained bands in IR spectra for Er^{3+} which indicates that the Er^{3+} ions enter in the interstitial sites of the network. From the IR studies, the number of non-bridging oxygens (NBOs) increase, which leads to loosening of structure with increase in the Bi_2O_3 content up to 25 mol%, and this is inconsistent with the data obtained from glass transition temperature.

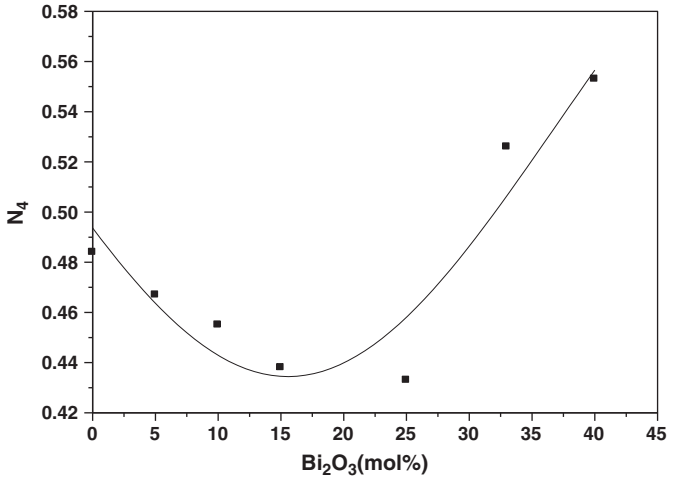

Fig. 14. Variation of N_4 with composition of Bi_2O_3 content.

4. Conclusions

The glass system under investigation has been prepared by conventional melt-quenching technique. The obtained results allow concluding that:

- The XRD data confirm the amorphous nature of the prepared samples.
- The optical band gap energy (E_g) decreases with increasing Bi_2O_3 content. This may be attributed to the formation of non-bridging oxygen (NBO). It is observed that (ΔE) increases with increasing Bi_2O_3.
- It is observed that the density (ρ) increases with increasing Bi_2O_3 content. This increase in density is mainly due to the difference in the atomic masses and atomic radii of Bi and B ions.
- The oxygen packing density (OPD) decreases as the concentration of Bi_2O_3 content increases. This indicates that the glass network becomes less tightly packed and the degree of disorder increases with the increase of concentration of Bi_2O_3.
- It is observed that, both electronic polarizability and optical basicity are increasing linearly by increasing the Bi_2O_3 content This is mainly due to the fact that Bi_2O_3 has a higher polarizability and higher optical basicity (due to its larger ionic radii) than Na_2O, Er_2O_3 and B_2O_3.
- DSC measurements were carried out to determine the glass transition temperature (T_g) of the glass samples. T_g is found to decrease with Bi_2O_3 content up to 25 mol%, and then increase with the increase of Bi_2O_3 content, which is due to rigid glass structure.
- IR spectra of present glass system are containing different band characteristics for BO_3, BO_4, BiO_3 and BiO_6 structural units.
- The ratio N_4 decreases by increasing Bi_2O_3 in the first five samples revealing the transformation of $BO_4 \rightarrow BO_3$ and then increases revealing the transformation of $BO_3 \rightarrow BO_4$.

References

[1] N. Srinivasa, M. Purnima, S. Bale, Bull. Mater. Sci. 29 (2006) 365–370.
[2] E.A. dos Santosa, L.C. Courrola, L.R.P. Kassaba, J. Lumin. 124 (2007) 200–206.
[3] S. Tanabe, J. Alloys Compd. 408–412 (2006) 675.
[4] L.R.P. Kassab, N.D.R. Junior, S.L. Oliveira, J. Non-Cryst. Solids 352 (2006) 3224.
[5] M. Boscaa, L. Pop, G. Borodi, P. Pascuta, J. Alloys Compd. 479 (2009) 579–582.
[6] H. Doweidar, Y.B. Saddeek, J. Non-Cryst. Solids 355 (2009) 348–354.
[7] D. Saritha, Y. Markandeya, et al., J. Non-Cryst. Solids 354 (2008) 5573–5579.
[8] Y.B. Saddeeka, M.S. Gaafarb, Mater. Chem. Phys. 115 (2009) 280–286.
[9] K. Boonin, J. Kaewkhao, T. Ratana, P. Limsuwan, Procedia Eng. 8 (2011) 207–211.
[10] Y.B. Saddeek, I.S. Yahia, K.A. Aly, W. Dobrowolski, Solid State Sci. 12 (2010) 1426e–1434e.
[11] V.T. Adamiv, Ya.V. Burak, R.V. Gamernyk, Funct. Mater. 18 (3) (2011).
[12] Y. Cheng, H. Xiao, W. Guo, Ceram. Int. 34 (2008) 1335–1339.
[13] L. Srinivasa Rao, M. Srinivasa Reddy, M.V. Ramana Reddy, N. Veeraiah, Physica B 403 (2008) 2542–2556.
[14] P. Pascuta, S. Rada, G. Borodi, M. Bosca, L. Pop, E. Culea, J. Mol. Struct. 924–926 (2009) 214–220.
[15] J.G. Sole, L.E. Bausa, D. Jaque, An Introduction to the Optical Spectroscopy of Inorganic Solids, John Wiley & Sons Ltd, England, 2005.
[16] G. Liu, B. Jacquier, Springer Series in Materials Science, , 2005.
[17] E.A. Davis, N.F. Mott, Philos. Mag. 22 (1970) 903–922.
[18] F. Urbach, Phys. Rev. 92 (1953) 1324.
[19] M. Subhadra, P. Kistaiah, Physica B 406 (2011) 1501–1505.
[20] S. Sindhu, S. Sanghi, A. Agarwal, V.P. Seth, N. Kishore, Mater. Chem. Phys. 90 (2005) 83.
[21] Y.B. Saddeek, E.R. Shaaban, E. Moustafa, H.M. Moustafa, Physica B 403 (2008) 2399–2407.
[22] E. Moustafa, Y.B. Saddeek, E.R. Shaaban, J. Phys. Chem. Solids 69 (2008) 2281–2287.
[23] G. Gao, L. Hu, H. Fan, G. Wang, K. Li, S. Feng, S. Fan, H. Chen, Opt. Mater. 32 (2009) 159–163.
[24] S. Mohan, K.S. Tined, G. Sharma, J. Phys. 37 (2007) 4.
[25] A.S. Rao, Y.N. Ahammed, R.R. Reddy, T.V.R. Rao, Opt. Mater. 10 (1998) 245–252.

[26] B. Kim, E. Lim, J. Lee, J. Kim, J. Eur. Ceram. Soc. 27 (2007) 819–824.
[27] S. Bale, S. Rahman, A. Awasthi, V. Sathe, J. Alloys Compd. 460 (2008) 699–703.
[28] B.C. Tischendorf, T.M. Alam, R.T. Cygan, J.U. Otaigbe, J. Non-Cryst. Solids 316 (2003) 261–272.
[29] X. Zhao, X. Wang, H. Lin, Z. Wang, Physica B 390 (2007) 293–300.
[30] J.A. Duffy, M.D. Ingram, J. Non-Cryst. Solids 21 (1976) 373.
[31] J. Duffy, M. Ingram, J. Am. Chem. Soc. 93 (1971) 6448.
[32] A. Murali, J. Lakshmana Rao, A. Venkata Subbaiah, J. Alloys Compd. 257 (1997) 96–103.
[33] S. Sindhu, S. Sanghi, A. Agarwal, V.P. Seth, N. Kishore, Spectrochim. Acta A 64 (2006) 196–204.
[34] J.A. Duffy, Bonding, Energy Levels and Bands in Inorganic Solids, Longmann, London, 1990.
[35] R.R. Reddy, Y. Nazeer Ahmmed, P. Abdul Azeem, K. Rama Gopal, T.V.R. Rao, J. Non-Cryst. Solids 286 (2001) 169–180.
[36] B. Karthikeyan, R. Philip, S. Mohan, Opt. Commun. 246 (2005) 153–162.
[37] B. Karthikeyan, S. Mohan, Physica B 334 (2003) 298–302.
[38] K. Błaszczak, A. Adamczyk, M. We˛dzikowska, M. Rokita, J. Mol. Struct. 704 (2004) 275–279.
[39] K. Błaszczak, A. Adamczyk, J. Mol. Struct. 596 (2001) 61–68.
[40] K. Błaszczak, W. Jelonek, A. Adamczyk, J. Mol. Struct. 511–512 (1999) 163–166.
[41] H. Doweidar, Y.B. Saddeek, J. Non-Cryst. Solids 356 (2010) 1452–1457.
[42] E.I. Kamitsos, A.P. Patsis, M.A. Karakassides, G.D. Chryssikos, J. Non-Cryst. Solids 126 (1990) 52.
[43] T. Rao, Ch. Reddy, Ch. Krishna, U. Thampy, R. Raju, P. Rao, R. Ravikumar, J. Non-Cryst. Solids 357 (2011) 3373–3380.
[44] P. Pascuta, G. Borodi, E. Culea, J. Non-Cryst. Solids 354 (2008) 5475–5479.